

# Function and subnuclear distribution of Rpp21, a protein subunit of the human ribonucleoprotein ribonuclease P

NAYEF JARROUS,<sup>1</sup> ROBERT REINER,<sup>1</sup> DONNA WESOLOWSKI,<sup>2</sup> HAGIT MANN,<sup>1</sup>  
CECILIA GUERRIER-TAKADA,<sup>2</sup> and SIDNEY ALTMAN<sup>2</sup>

<sup>1</sup>Department of Molecular Biology, The Hebrew University-Hadassah Medical School, Jerusalem 91120, Israel

<sup>2</sup>Department of Molecular, Cellular and Developmental Biology, Yale University, New Haven, Connecticut 06520, USA

## ABSTRACT

Rpp21, a protein subunit of human nuclear ribonuclease P (RNase P) was cloned by virtue of its homology with Rpr2p, an essential subunit of *Saccharomyces cerevisiae* nuclear RNase P. Rpp21 is encoded by a gene that resides in the class I gene cluster of the major histocompatibility complex, is associated with highly purified RNase P, and binds precursor tRNA. Rpp21 is predominantly localized in the nucleoplasm but is also observed in nucleoli and Cajal bodies when expressed at high levels. Intron retention and splice-site selection in Rpp21 precursor mRNA regulate the intranuclear distribution of the protein products and their association with the RNase P holoenzyme. Our study reveals that dynamic nuclear structures that include nucleoli, the perinucleolar compartment and Cajal bodies are all involved in the production and assembly of human RNase P.

**Keywords:** Cajal bodies; nucleolus; precursor tRNA; ribonuclease MRP; ribonuclease P

## INTRODUCTION

Processing of the 5' leader sequences of precursor tRNAs requires the ribonucleoprotein enzyme ribonuclease P (RNase P; Frank & Pace, 1998; Altman & Kirsebom, 1999). As do eubacterial RNase P enzymes, eukaryotic nuclear RNase P has both indispensable RNA and protein subunits in vivo (Chamberlain et al., 1998). However, the protein subunits are also essential for catalysis in vitro (Pfeiffer et al., 2000; Thomas et al., 2000), unlike the case of eubacterial RNase P (Altman & Kirsebom, 1999).

Nuclear RNase P from *Saccharomyces cerevisiae* has at least nine protein subunits (Chamberlain et al., 1998) that are essential for processing of precursor tRNA (Lygerou et al., 1994; Chu et al., 1997; Dichtl & Tollervy, 1997; Stolc & Altman, 1997; Chamberlain et al., 1998; Stolc et al., 1998). Except for Rpr2p, the protein subunits of this holoenzyme are shared with RNase MRP (Chamberlain et al., 1998), a mitochondrial and ribosomal RNA processing ribonucleoprotein

enzyme (Lygerou et al., 1996a; Lee & Clayton, 1997). Purification of nuclear RNase P from HeLa cells shows that this ribonucleoprotein also possesses numerous protein subunits (Lygerou et al., 1996b; Eder et al., 1997; Jarrous et al., 1998, 1999a; Jarrous & Altman, 2001). Homologs of subunits are found in yeast and shared with RNase MRP (Lygerou et al., 1996b; Pluk et al., 1999; van Eenennaam et al., 1999), but their functions in enzyme activity and tRNA recognition have not been demonstrated.

The precise locale of active RNase P within the nucleus is not well defined. The RNA subunit, H1 RNA, of the holoenzyme is dispersed in the cell nucleoplasm in mammalian cells, but is also localized in the nucleolus, the perinucleolar compartment and, to some extent, the cytoplasm (Matera et al., 1995; Lee et al., 1996; Jacobson et al., 1997; Wolin & Matera, 1999). In contrast, several Rpp subunits, including Rpp14, Rpp29, and Rpp38, are mainly localized in the nucleolus (Jarrous et al., 1999b). Rpp14 and Rpp29 are confined to the dense fibrillar component, the site of early processing of rRNA (Shaw et al., 1995) and of the subunit hPop1 (Lygerou et al., 1996b). Moreover, Rpp29 and Rpp38 also exhibit punctate distribution in the nucleus, an indication that these proteins are not restricted to

Reprint requests to: Nayef Jarrous, Department of Molecular Biology, The Hebrew University-Hadassah Medical School, Jerusalem 91120, Israel; e-mail: jarrous@md.huji.ac.il.

nucleoli. These two subunits exist in Cajal (coiled) bodies (Jarrous et al., 1999b), nuclear structures enriched with components of transcription complexes and small nuclear and nucleolar ribonucleoproteins involved in processing of mRNA and rRNA (Lamond & Earnshaw, 1998; Gall et al., 1999). Thus, distinct nuclear bodies, which form at sites of high activity of gene transcription and RNA processing (Gall et al., 1999; Lewis & Tollervy, 2000; Pederson, 2000), participate in the biogenesis of tRNA (Jarrous et al., 1999b).

The nucleolus may serve as an assembly site for RNase P and a place for its association with a putative, large ribonucleoprotein that consists of ribosome subunits, the signal recognition particle, and 5S ribonucleoproteins (Pederson & Politz, 2000). In *S. cerevisiae*, there is evidence that both the majority of the RNase P RNA is found in the nucleolus and 5' processing of some precursor tRNAs may occur in this structure (Bertrand et al., 1998; Kendall et al., 2000). Together, these findings raised the possibility that 5' processing of precursor tRNA is a conserved nucleolar function (Lewis & Tollervy, 2000).

We here characterize Rpp21, a protein subunit of catalytic complexes of human RNase P, and show that it functions in binding of precursor tRNA. The production of Rpp21 and that of a related protein, Rpp21i, which is not associated with the holoenzyme, is determined by a unique mRNA splicing variation mechanism. In contrast to previously characterized Rpp subunits, which are primarily found in nucleoli and Cajal bodies, Rpp21 is mainly dispersed in the cell nucleoplasm. We suggest that several dynamic compartments, which include nucleoli, Cajal bodies, and the perinucleolar compartment, participate in the production and assembly of nuclear RNase P in human cells.

## RESULTS

### Characterization of Rpp21, a protein encoded by a gene that resides in the MHC locus

In *S. cerevisiae*, nuclear RNase P has a protein subunit termed Rpr2p (Chamberlain et al., 1998). Using the sequence of Rpr2p in database BLAST programs (Altschul et al., 1997), we found several corresponding human expressed sequence tag (EST) clones (see Materials and Methods). From these ESTs, a clone with a cDNA insert of ~0.6 kb in length was fully sequenced and found to have an open reading frame that theoretically codes for polypeptide of 154 amino acids and exhibits 23% identity with Rpr2p (Fig. 1A). This protein, designated Rpp21, has a predicted molecular weight of 17,570 Da with a pI of 9.64. A distinctive cysteine arrangement, CX<sub>2</sub>CX<sub>9</sub>CX<sub>6</sub>CX<sub>9</sub>CX<sub>2</sub>C (where X is any amino acid and the numbers refer to the number of

amino acids between cysteines) spans positions 62 to 95 of this polypeptide (Fig. 1A).

Using the sequence of the *RPP21* cDNA described above, we found an *RPP21* gene candidate in a fully sequenced, human genomic DNA fragment of 46,681 bp derived from position 6p21 of chromosome 6 (Janer & Geraghty, 1998; accession no. AC004187). This position is the genetic locus of the class I gene cluster of the major histocompatibility complex (Janer & Geraghty, 1998; Shiina et al., 1999). According to a known transcription map of this locus, the *RPP21* gene corresponds to an anonymous clone, termed CAT 60, that is located in position 6p21.3, nearby the *HLA-E* gene (Gruen et al., 1996). Comparative analysis of the *RPP21* cDNA sequence (Fig. 1A) with that of the genomic MHC DNA fragment described above revealed that *RPP21* is ~2 kb in length and has five exons and four introns (Fig. 2B; see below).

Some other EST clones, which exhibited identity to the 5' sequence of *RPP21* cDNA, have been found to possess an additional 69 nt that separate exon 1 from exon 2 (data not shown; accession no. AA335783). These intervening 69 nt correspond to the entire intron 1 of *RPP21* (Fig. 2B). Thus, intron 1 appears to be retained in some mRNAs and potentially codes for 23 amino acids that can be introduced in-frame in a new, putative polypeptide (Fig. 1B). Unexpectedly, sequence analysis of cDNA clones that contained intron 1 showed that retention of intron 1 was accompanied by alternative splicing of exon 4. This alternative splicing occurred 7 nt downstream from the normal 5' splice site of exon 4 (Fig. 2A). Insertion of these intronic 7 nucleotides in mRNA altered the downstream open reading frame and introduced a stop codon upstream from the original stop codon found in exon 5 (Fig. 1B). The cDNA with the retained intron has an open reading frame that potentially codes for a polypeptide, designated Rpp21i, of 167 amino acids with a predicted molecular weight of 18,992 Da and a pI of 10.74 (Fig. 1B). The domain of 23 amino acids encoded by intron 1, encompassing positions 20 to 41 of Rpp21i, has numerous arginine and proline residues (Fig. 1B). The cysteine arrangement CX<sub>2</sub>CX<sub>9</sub>CX<sub>6</sub>CX<sub>9</sub>CX<sub>2</sub>C encompasses positions 85 to 118 of Rpp21i (Fig. 1B).

The *RPP21* and *RPP21i* cDNAs described above were subcloned in pHTT7K and overexpressed in *Escherichia coli* as histidine-tagged proteins (see Materials and Methods). The overexpressed Rpp21 and Rpp21i proteins were found in inclusion bodies and therefore they were solubilized in urea, purified on nickel-charged resin columns, and then dialyzed to eliminate the denaturant. Recombinant Rpp21 and Rpp21i migrated in 12% polyacrylamide/SDS gels as 24- and 22-kDa proteins, respectively (Fig. 1C). When compared to their theoretical molecular weights, Rpp21, but not Rpp21i, has a slightly anomalous migration in the gel after taking into account the extra 2 kDa of the histidine tag.

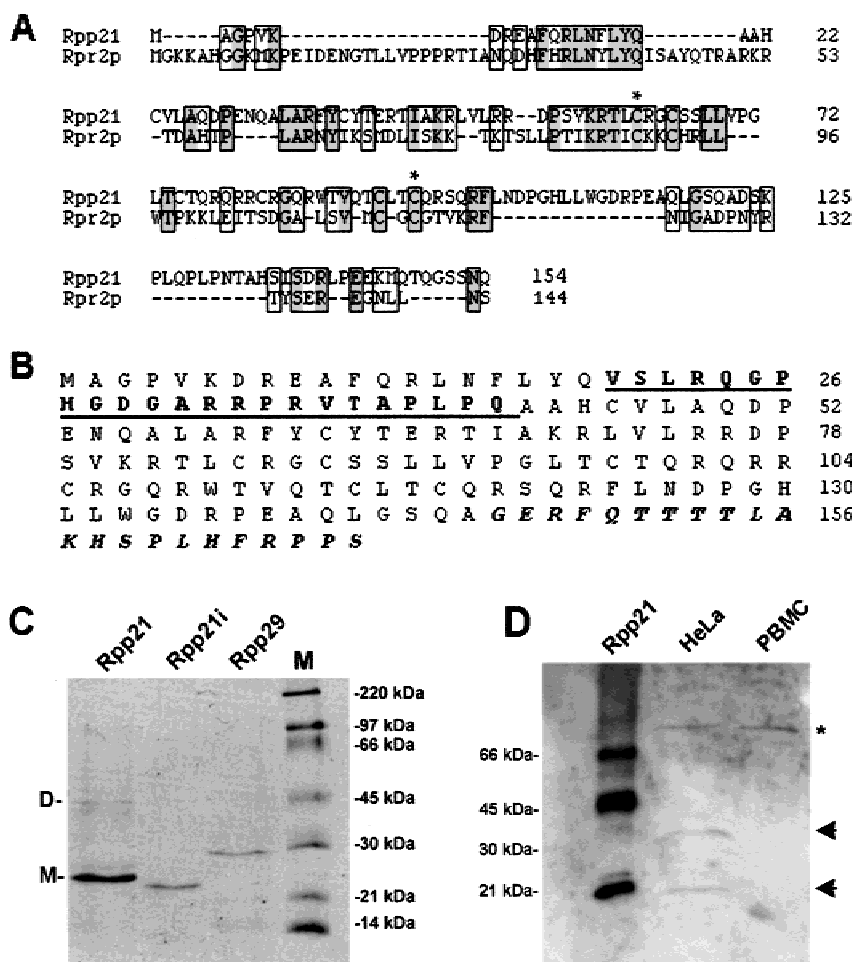


**FIGURE 1.** Characterization of Rpp21 and Rpp21i. **A:** Alignment of amino acid sequence of Rpp21 with the yeast Rpr2p. Amino acids are numbered from the first methionine residue. Identical amino acids in both polypeptides are shown in shaded boxes. Twenty-three percent of residues are identical in both proteins. Amino acids with conserved properties are boxed. The two asterisks mark the first and last residues in the cysteine cluster  $CX_2CX_9CX_6CX_9CX_2C$  that spans positions 62 to 95 of Rpp21. **B:** Amino acid sequence of Rpp21i. The 23 amino acids from positions 20 to 42, which are encoded by intron 1, are highlighted in bold and underlined letters. The carboxy terminal 22 amino acids of Rpp21i, which result from translation of alternatively spliced mRNA, are shown in bold and italic letters. **C:** Histidine-tagged Rpp21 and Rpp21i proteins overexpressed in *E. coli* were affinity purified on nickel-charged His-Bind resin columns and eluted proteins were separated in 12.5% PAGE/SDS and then stained by Coomassie blue. M and D correspond to monomers and dimers of recombinant Rpp21. Highly purified, histidine-tagged Rpp29 and a protein size marker are shown. **D:** Polyclonal antibodies raised against a synthetic peptide that corresponds to the C-terminal 23 amino acids of Rpp21 recognize in western blot analysis, the recombinant Rpp21 polypeptide (24 kDa with the extra histidine tag; first lane) and a 21-kDa protein in crude extracts of HeLa cells (second lane). Rpp21 in PBMC (third lane) was barely seen when compared to HeLa cells. Recombinant Rpp21 forms dimers and trimers detected by the antibody. Asterisk may represent a nonspecific, cross-reacted protein.

### Rpp21 and Rpp21i are products of intron retention and splice-site selection

We studied expression of mRNAs that coded for both Rpp21 and Rpp21i in human tissue culture cells. Thus, total RNA (50  $\mu$ g) extracted from HeLa cells and human peripheral blood mononuclear cells (PBMCs; see Materials and Methods) was subjected to quantitative RNase protection analysis using specific, antisense RNA probes, P3 and P5 (Fig. 2C). The P5 probe covers adjacent exon 1, intron 1, exon 2, exon 3, and part of exon 4 of the Rpp21i mRNA (Fig. 2C). In both HeLa cells and mononuclear cells, P5 protected a major RNA of 190 nt in length that corresponds to Rpp21 mRNA with exons 2, 3, and 4 being fully spliced (Fig. 2A; lanes 4 and 5; lower arrow). In addition, RNA of 316 nt in length was detected (Fig. 2A; lanes 4 and 5; top arrow). This 316-nt RNA corresponds to Rpp21i mRNA that contains the retained intron 1 between exon 1 and exon 2 (Fig. 2A). Smaller RNAs (<190 nt) may represent partially excised precursor mRNA intermediates (Fig. 2A; lanes 4 and 5).

The aforementioned results were corroborated with the use of probe P3, which covers exon 1, exon 2,

exon 3, and part of exon 4 of Rpp21 mRNA (Fig. 2C). The P3 RNA probe protected a major RNA of 259 nt that represents Rpp21 mRNA with four exons being fully spliced (Fig. 2A; lanes 2 and 3; upper arrow). The shorter RNA of 190 nt corresponds to Rpp21i mRNA with exons 2–4 fully spliced, as is also the case with the RNA of 190 nt mentioned above (Fig. 2A, lanes 2 and 3; lower arrow).

The quantitative RNA analyses described above show a ratio of 5:1 between Rpp21 and Rpp21i mRNAs (Fig. 2A). Of note, Rpp21 and Rpp21i mRNAs are more abundant in HeLa cells than in resting human peripheral blood mononuclear cells (Fig. 2A; lane 4 versus 5), suggesting that expression of Rpp21 is induced in transformed HeLa cells.

Polyclonal antibodies raised against a synthetic peptide that corresponds to the C-terminal 23 amino acids of Rpp21 recognize, in western blot analysis, a 21-kDa protein in crude extracts of HeLa cells, as well as the recombinant Rpp21 polypeptide (Fig. 1D; see below). Rpp21 in PBMC was barely seen when compared to HeLa cells (Fig. 1D), consistent with the observed low expression of the Rpp21 mRNA in PBMCs (Fig. 2A). We were unable to detect Rpp21i in HeLa cell crude

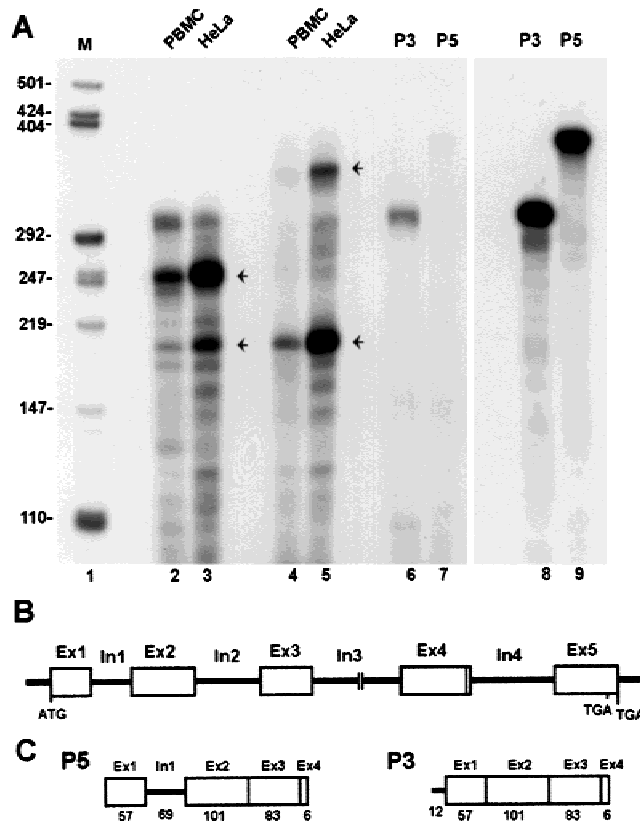


**FIGURE 2.** Expression of Rpp21 and Rpp21i mRNAs and retention of intron 1. **A:** Total RNA (50  $\mu$ g) extracted from HeLa cells or human peripheral mononuclear cells (PBMC) was subjected to RNase P protection analysis using two internally  $^{32}$ P-labeled RNA probes, P3 (lanes 2 and 3) and P5 (lanes 4 and 5). The P3 probe covers joint exon 1 to exon 4. Protected RNAs of 259 and 190 nt are indicated by arrows (lanes 2 and 3). Protected RNAs of 316 and 190 nt are noted by arrows (lanes 4 and 5). The P5 probe covers exon 1, intron 1, exon 2, exon 3, and exon 4. Intact (lanes 8 and 9) and RNase-treated (lanes 6 and 7) P3 and P5 RNAs were also separated in the same 5% polyacrylamide/7 M urea gel. A short exposure of the two intact P3 and P5 RNA probes (lanes 8 and 9) is shown. As a size marker (M; lane 1), pGEM-3 was digested by *MspI* and labeled in a filling-in reaction using  $^{32}$ P-dCTP. **B:** Schematic map of *RPP21* gene that contains five exons and four introns. Small box in exon 4 represents 7 nt introduced in the alternatively spliced Rpp21i mRNA. ATG presents initiation of translation and the two TGA triplets in exon 5 indicate the stop codons of Rpp21i and Rpp21, respectively. **C:** Schematic maps of the cDNA fragments used to prepare the P3 and P5 RNA probes.

extracts using antibodies raised against a synthetic peptide deduced from the 23 amino acids encoded by intron 1 (Fig. 1B), although these polyclonal antibodies recognized their corresponding, recombinant Rpp21i polypeptide (data not shown). However, HeLa cells can express exogenous, tagged Rpp21i protein derived from fusion constructs (see below).

### Rpp21 but not Rpp21i is associated with catalytically active RNase P

RNase P was purified from HeLa cells through the glycerol gradient step (Eder et al., 1997) and fractions across

the peak of enzyme activity (Fig. 3A) were subjected to western blot analysis using antibodies against Rpp21 (see Materials and Methods). These antibodies recognized a 21-kDa protein (Rpp21) that copurified with RNase P (Fig. 3B). The RNase P subunits, Rpp29 and Rpp14 (Jarrous et al., 1999a), also copurified with Rpp21 and the enzyme activity (Figs. 3C–E). Immunoprecipitation assays demonstrated that anti-Rpp21 antibodies effectively brought down RNase P that was active in processing of precursor tRNA (Fig. 3F). By contrast, anti-Rpp21i antibodies did not recognize their corresponding protein in the above fractions or precipitate active RNase P from crude extracts of HeLa cells or from partially purified preparations of this holoenzyme (not shown). These results indicate that Rpp21, but not Rpp21i, is a subunit of catalytically active RNase P.

### Recombinant Rpp21 binds to precursor tRNA in vitro

Gel shift analysis showed that highly purified recombinant Rpp21, eluted from a nickel-charged column (Fig. 4A) was able to bind precursor tRNA<sup>Tyr</sup> in vitro (Fig. 4B; see Materials and Methods). The binding reactions were carried out in a buffer that contained 450 mM NaCl to eliminate nonspecific binding of this positively charged polypeptide to precursor tRNA. Of note, binding to precursor tRNA was obtained with fractions F4 to F6 that contained dimers and trimers of recombinant Rpp21 (Fig. 4, A versus B). In addition to Rpp21, we found that highly purified, recombinant Rpp14 (Jarrous et al., 1999a) was also capable of binding precursor tRNA<sup>Tyr</sup> (Fig. 4C). The binding of Rpp21 and Rpp14 to precursor tRNA was blocked by a 100-fold excess of unlabeled precursor tRNA<sup>Tyr</sup> but not by poly I:C, a nonspecific RNA competitor (Fig. 4C). In contrast to Rpp14 and Rpp21, highly purified, recombinant Rpp20, Rpp29, Rpp30, Rpp38, and Rpp40 (Jarrous et al., 1998, 1999a) failed to bind to precursor tRNA<sup>Tyr</sup> (Fig. 4C) or yeast precursor tRNA<sup>Ser</sup> (*pSupS1*) (data not shown) under the same conditions. These findings demonstrate that recombinant Rpp21 and Rpp14 selectively bind to precursor tRNA, and demonstrate the involvement of two protein subunits of human RNase P in substrate recognition.

### Localization of Rpp21 in the cell nucleoplasm

We previously demonstrated that several protein subunits of human RNase P, including Rpp29 and Rpp38, are primarily localized in nucleoli and Cajal bodies of HeLa cells and of transfected Swiss 3T3 fibroblasts (Jarrous et al., 1999b). To obtain more information regarding the intracellular locale of Rpp21, we examined its distribution in HeLa cells. Cells were transiently transfected with a pEGFP-Rpp21 construct, in which the

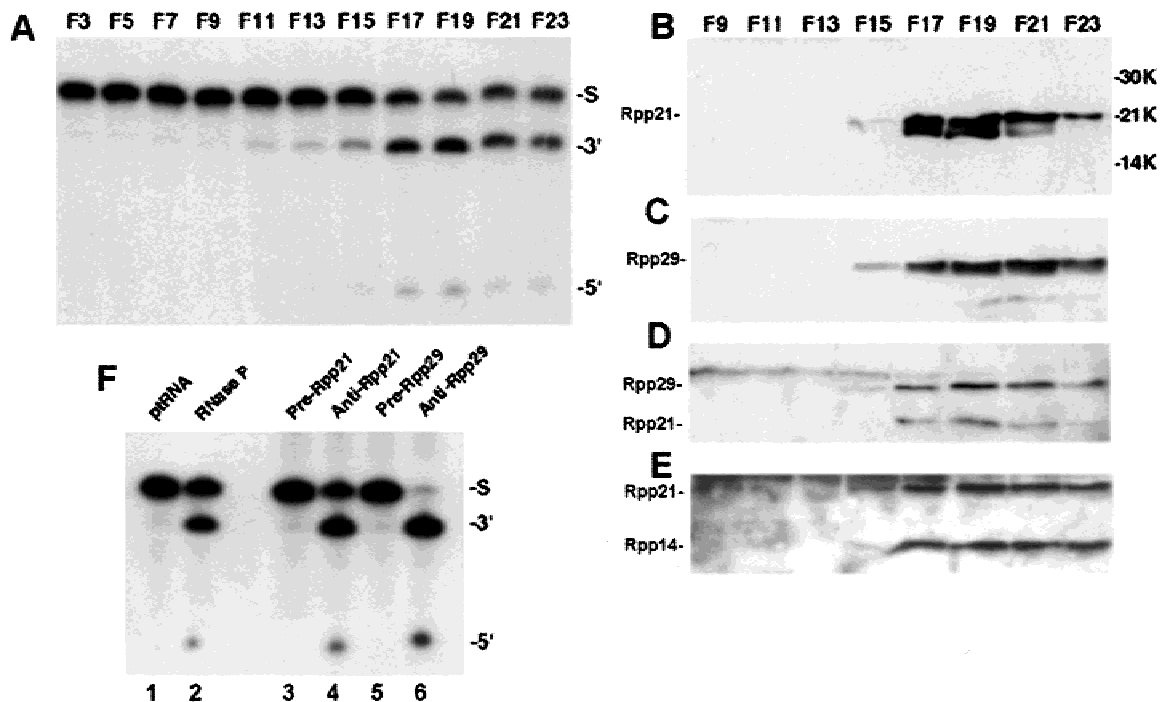


**FIGURE 3.** Rpp21 is a subunit of active nuclear RNase P ribonucleoproteins. **A:** Fractions (F3–F23) from a 15–35% glycerol gradient were tested for RNase P activity in processing of precursor tRNA<sup>Ser</sup> (*pSupS1*) (S). RNase P reactions were carried out in 1×PA buffer (see Materials and Methods) for 2 min at 37 °C and the cleavage products, mature tRNA (3′) and 5′ leader sequence (5′), were separated on 8% polyacrylamide/7 M urea gel. **B–E:** Proteins in fractions F9–F23 were separated in 12% SDS/PAGE and subjected to western blot analysis using polyclonal rabbit antibodies raised against Rpp21 (**B**), Rpp29 (**C**), Rpp21 and Rpp29 (**D**), or Rpp21 and Rpp14 (**E**). **F:** Immunoprecipitation of active HeLa RNase P. Aliquots of 10 μL from the fraction with the peak of RNase P activity shown in fraction F19 were subjected to immunoprecipitation analysis using Protein A beads coupled to rabbit antisera against Rpp21 (lane 4) or Rpp29 (lane 6; Jarrous et al., 1999a). Immunoprecipitates were tested for RNase P activity on precursor tRNA<sup>Ser</sup> as described above. RNase P activity in precipitates obtained with beads coupled to the preimmune sera of the rabbits before immunization with Rpp21 (lane 3) or Rpp29 (lane 5) was tested. Control reactions of precursor tRNA<sup>Ser</sup> incubated with (lane 2) and without (lane 1) HeLa RNase P are shown.

Rpp21 open reading frame was fused to green fluorescent protein (GFP), and were observed 24 h later with a confocal fluorescence microscope (see Materials and Methods). GFP-Rpp21 was localized primarily in the cell nucleoplasm (Fig. 5A–D). Although GFP-Rpp21 was not equally distributed in the nucleoplasm, no prominent punctate staining was visible (Fig. 5B), suggesting that this subunit is diffused in this compartment. However, some GFP-Rpp21 was also seen in islands in the nucleoli (Fig. 5B). In three transfection experiments, we found that in 70% of transfected cells, GFP-Rpp21 was retained in the nucleoplasm, whereas in 30% of the cases, this fusion protein was also localized in nucleoli. GFP alone was visible in the cytoplasm and was excluded from nucleoli (data not shown; Jarrous et al., 1999b). In transfected HeLa cells that showed strong GFP-Rpp21 signal (Fig. 5F; compare cells indicated by green and red arrows) the fusion protein accumulated in nucleoli (Fig. 5E–H). This suggests that GFP-Rpp21 may be retained in the nucleoplasm by a limiting factor. As judged by indirect immunofluorescence analysis using anti-Rpp21 antibodies, endogenous Rpp21 is predominantly localized in the nucleoplasm, and only a

small fraction of it enters nucleoli (Fig. 5B, insert, green arrow), thereby consistent with the results obtained with GFP-Rpp21 expressed at low levels in transfected cells. Because both endogenous Rpp21 and GFP-Rpp21 are dispersed in the nucleoplasm, it was difficult to determine whether these proteins were localized in Cajal bodies that were immunostained with antibodies against p80-coilin (inserts in Fig. 5B,C, and Fig. 5D,H, yellow). However, in both cases, these proteins were not concentrated in Cajal bodies.

Our results indicate that Rpp21 is primarily localized in the nucleoplasm, when not expressed at high levels, in contrast to some other previously characterized Rpp subunits, including Rpp29 and Rpp38 that are mainly found in nucleoli and Cajal bodies (Jarrous et al., 1999b).

#### Differential distribution of Rpp21i in the nucleus

We next examined the intracellular distribution of Rpp21i. Swiss 3T3 fibroblasts were transiently transfected with pEGFP-Rpp21i, in which the open reading frame of Rpp21i cDNA was fused to the carboxy terminal of

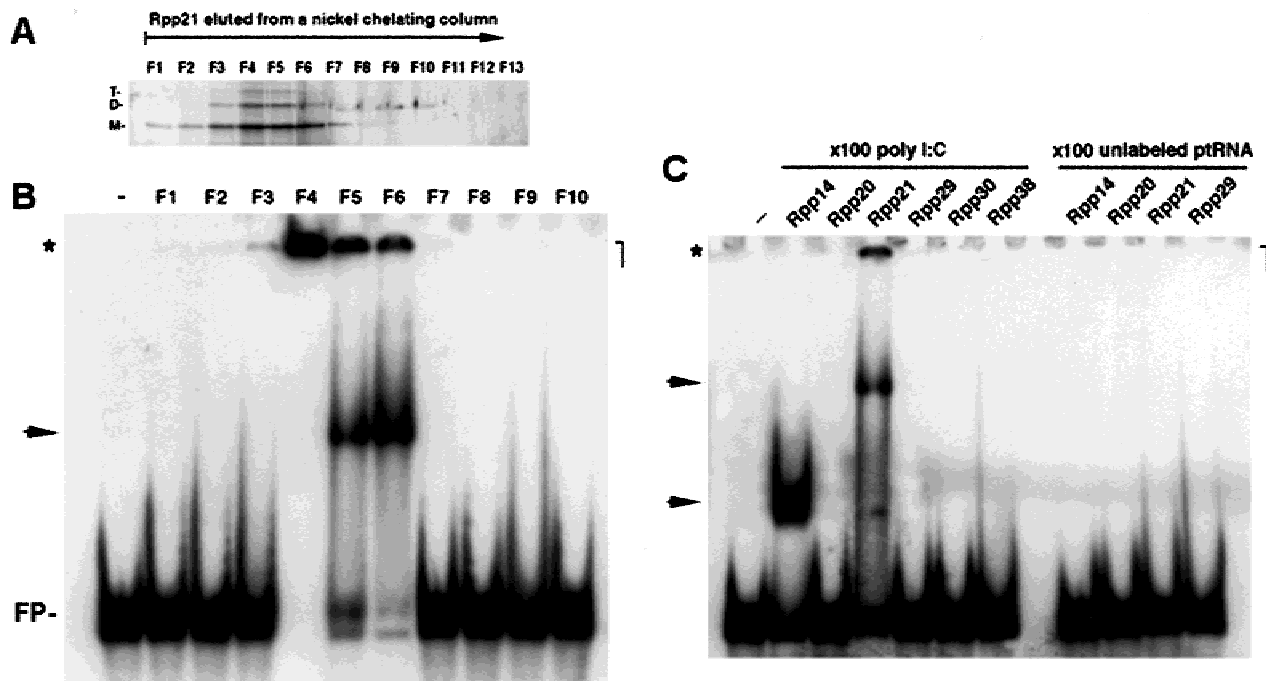


**FIGURE 4.** Rpp21 and Rpp14 bind precursor tRNA. **A:** Silver stain of recombinant Rpp21 protein in fractions F1 to F13 eluted from a nickel-charged resin (see Materials and Methods). M, D, and T represent monomers, dimers, and trimers of the recombinant protein. **B:** Five micrograms from each of fractions F1 to F10 described above were incubated with 5 pmol of labeled precursor tRNA<sup>Tyr</sup> in the presence of excess amount (100-fold) of poly I:C RNA. After 20 min at 37 °C, complexes were separated in 5% native polyacrylamide gel. An arrow indicates the RNA–protein complex. Signals (asterisk) seen in gel wells may represent large RNA–protein complexes resulting from polymerization of Rpp21. **C:** Labeled precursor tRNA<sup>Tyr</sup> was incubated with the indicated recombinant Rpp proteins (5  $\mu$ g each) in the presence of excess amount (100-fold) of poly I:C RNA or unlabeled precursor tRNA<sup>Tyr</sup>. Binding conditions and complex separation were carried out as for **B**.

GFP (Fig. 6A–C) or to a short myc tag detected by indirect immunofluorescence using the 9E10 monoclonal antibody (Fig. 6D–F). These fusion proteins were primarily localized in nucleoli of transfected fibroblasts (Fig. 6A–F). Myc-Rpp21i was concentrated in subnuclear sites (Fig. 6D–F) and colocalized with the endogenous fibrillar protein found in the dense fibrillar component (Fig. 6D–F). A similar pattern of intranuclear distribution has been observed in HeLa cells expressing myc-Rpp21i (Fig. 6G–K). However, myc-Rpp21i was not clearly seen in Cajal bodies, as judged by costaining of HeLa cells with anti-p80 coilin antibodies (Fig. 6J,K).

HeLa cells that showed high expression of myc-Rpp21i resulted in deformation of the regular structure of the nucleolus (Fig. 6G; note nucleoli in a transfected cell versus those in an untransfected one). Unexpectedly, colocalization studies of GFP-Rpp21i with endogenous Rpp29 showed that the latter protein was completely excluded from nucleoli in the transfected cells (Fig. 6L–N, yellow arrows). Transfection of cells with GFP fused to Rpp21 (Fig. 5A–D), Rpp14, Rpp29, or Rpp38, did not cause the exclusion of endogenous subunits from the nucleolus (Jarrous et al., 1999b; data not shown). The endogenous Rpp29, however, remained in the nucleoplasm of the transfected cells (Fig. 6N).

## DISCUSSION

We have characterized Rpp21, a protein subunit of the human tRNA processing enzyme, RNase P. Rpp21 is a positively charged polypeptide and shows moderate homology with Rpr2p, an essential protein subunit of *S. cerevisiae* nuclear RNase P (Chamberlain et al., 1998). As demonstrated by biochemical purification and immunoprecipitation analysis, Rpp21 is a subunit of catalytically active nuclear RNase P. Recombinant Rpp21, and another subunit, Rpp14, are capable of binding of precursor tRNA, thus showing for the first time that protein subunits of nuclear RNase P may have a role in substrate recognition. We further show that both the association of Rpp21 with RNase P and its intranuclear distribution are determined by alternative mRNA splicing.

### Rpp21 is encoded by a gene that resides in the MHC class I region and is regulated at processing of precursor mRNA

Rpp21 is encoded by a gene that is found in close proximity to the HLA-E gene in the class I gene cluster of the MHC locus. The HLA-E molecule modulates immune responses of natural killer cells (Braud et al.,

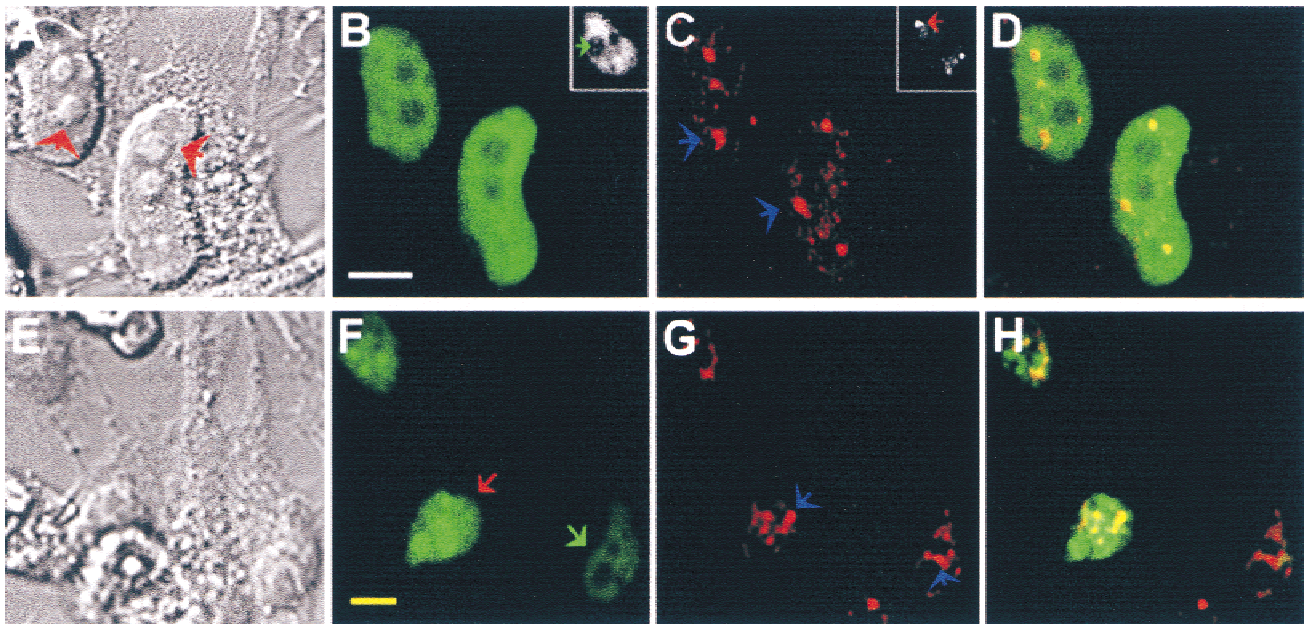


**FIGURE 5.** Intranuclear distribution of Rpp21. HeLa cells were transiently transfected for 24 h with pEGFP-Rpp21. Fixed cells were then subjected to indirect immunofluorescent analysis using antibodies against p80-coilin and examined with a confocal microscope (see Materials and Methods). Images of DIC (**A**), GFP signal (**B**), p80-coilin (**C**), and an overlay of **B** and **C** (**D**) are shown. Some of the GFP-Rpp21 and p80-coilin signal are seen in nucleoli. HeLa cells were analyzed for localization of endogenous Rpp21 (insert in **B**) using polyclonal rabbit antibodies raised against a synthetic Rpp21 peptide and p80-coilin (insert in **C**). A signal of endogenous Rpp21 is also seen in subnucleolar compartments (insert in **B**). Arrows in **A** point to nucleoli (Jarrous et al., 1999b). No specific signal above autofluorescent was observed when control sera of rabbits were tested (not shown). **E–H**: transfected HeLa cells that express high levels of GFP-Rpp21 show strong nucleolar signal (red arrow in **F**), whereas those that express lower levels exhibit mainly nucleoplasmic stain (green arrow in **F**) of this fusion protein. Images of DIC (**E**), GFP (**F**; green), p80-coilin (**G**; red), and overlay of **F** and **G** (**H**) are shown. Bars in **B** and **F** equal 5 and 10  $\mu\text{m}$ , respectively.

1998) and is linked to autoimmune diseases (Hodgkinson et al., 2000). It remains to be shown that Rpp21 serves as an autoantigen, as do other subunits of RNase P (Gold et al., 1989; Lygerou et al., 1996b; Eder et al., 1997) or is linked to cellular functions of the MHC system.

Expression of Rpp21 is regulated by processing of precursor mRNA by a mechanism that involves intron retention and differential splice-site selection. Retention of intron 1 is associated with the selection of an alternative 5' donor site of exon 4 in Rpp21 precursor mRNA. This association is supported by comparison of sequences of dbEST clones that contain *RPP21i*cDNAs (data not shown). Accordingly, retention of intron 1 may dictate the selection of a downstream cryptic splice site in intron 4 by a yet unknown splicing mechanism. The consequence of alternative mRNA splicing is the introduction of 7 nt from intron 4 into the 5' end of exon 5. This event frameshifts the downstream open reading frame of exon 5 and generates a new translation product, Rpp21i (Fig. 1B). Rpp21i is not associated with catalytically active RNase P, as judged by western blot analysis and immunoprecipitation assays of the holoenzyme using specific antibodies directed against the 23 amino acids encoded by intron 1. Thus, the distinct carboxy terminus and/or insertion of the 23 amino acids

encoded by intron 1 in Rpp21i appear to disrupt a domain responsible for inclusion in the RNase P holoenzyme complex. One of the common regions between Rpp21 and Rpp21i, however, is the cysteine arrangement  $\text{CX}_2\text{CX}_9\text{CX}_6\text{CX}_9\text{CX}_2\text{C}$  (Fig. 1A,B). This arrangement, which includes two CXXC thioredoxin-box motifs, may facilitate binding of metal ions, for example, zinc or iron-sulfur (Fe-S) clusters, required for catalytic and redox functions and iron homeostasis (Coldren et al., 1997; Beinert & Kiley, 1999).

#### The intranuclear partitioning of Rpp21 proteins is regulated by mRNA splicing variation

High levels of expression of GFP-Rpp21 in transfected HeLa cells results in accumulation of the fusion protein in the nucleolus rather than in the nucleoplasm (Fig. 5E–H). This observation indicates that Rpp21 is actively retained in the latter compartment of the nucleus most likely through interaction with another protein subunit or with nucleoplasmic H1 RNA, the RNA subunit of RNase P. By contrast, high intracellular concentration of GFP-Rpp14 caused massive accumulation of this fusion protein in the cytoplasm of HeLa cells (Jarrous et al., 1999b). Rpp14 and Rpp21 are ob-

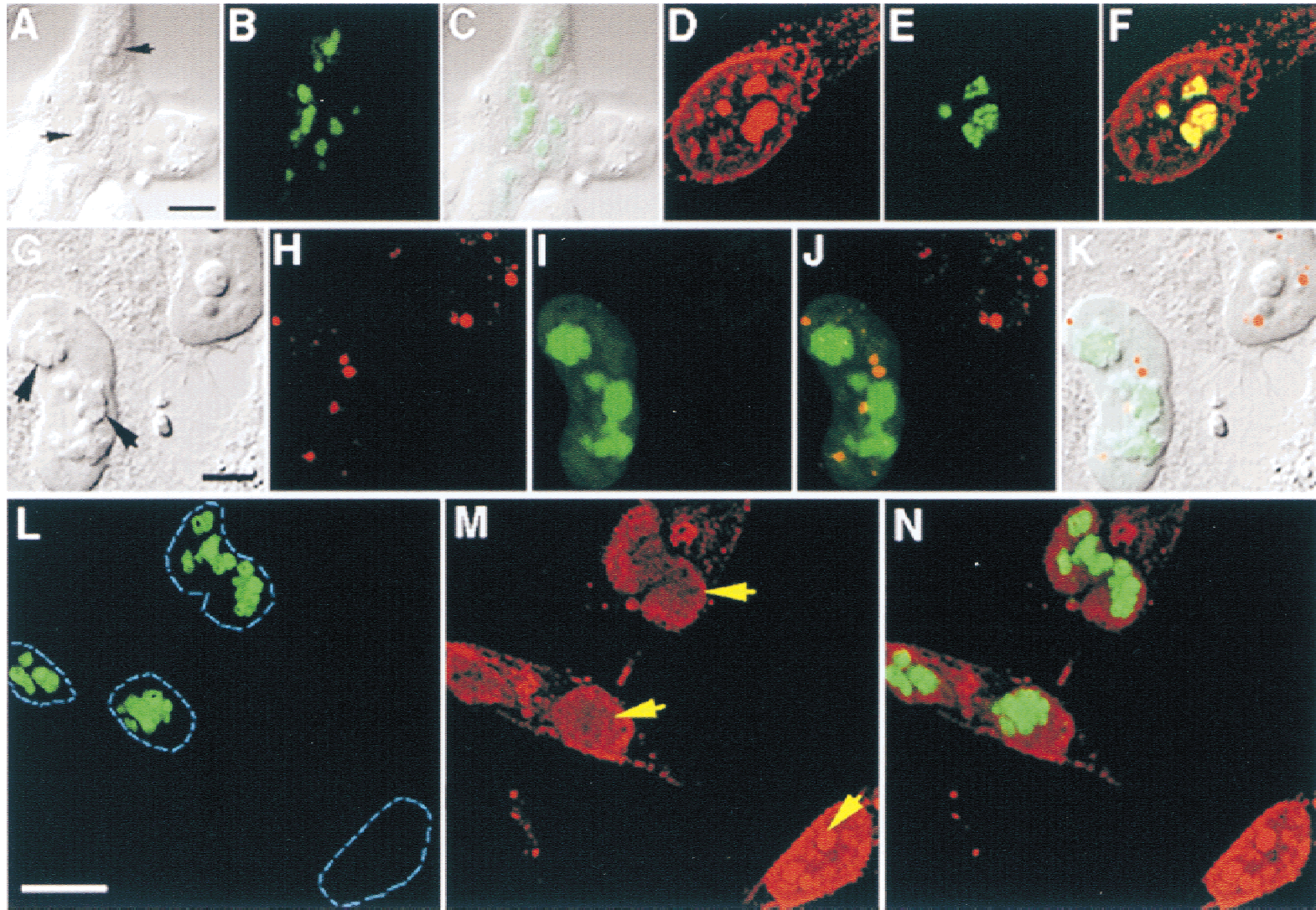


**FIGURE 6.** Differential localization of Rpp21i in the nucleus. Swiss 3T3 fibroblasts were transiently transfected with pEGFP-Rpp21i and after 24 h, living cells were examined with a confocal microscope (see Materials and Methods). Images of DIC (**A**), GFP signal (**B**; green), and an overlay of **A** and **B** (**C**) are shown. Arrows indicate two nucleoli. **D–F**: fixed Swiss 3T3 cells transfected with myc-Rpp21i were subjected to indirect immunofluorescent analysis using 9E10 (**D**) and anti-fibrillarin (**E**) monoclonal antibodies. The overlay of **D** and **E** is seen in **F**. **G–K**: HeLa cells were transfected for 24 h with myc-Rpp21i and then were fixed and stained with antibodies against p80-coilin. Images of DIC (**G**), p80-coilin (**H**), myc-Rpp21i (**I**), an overlay of **H** and **I** (**J**), and overlay of **G**, **H**, and **I** (**K**) are shown. Arrows in **G** point to deformed nucleoli compared to those visible in the nearby control cell. **L–N**: Swiss 3T3 fibroblasts were transfected for 24 h with GFP-Rpp21i and then were immunostained with anti-Rpp29 antibodies as described in Jarrous et al. (1999b). Images of GFP (**L**), Rpp29 (**M**), and overlay of **L** and **M** (**N**) are shown. Dashed lines demarcate cell nuclei and yellow arrows point to nucleoli. Rpp29 is seen in nucleoli only in untransfected cells (**M** and **N**; right side). Bars in **A**, **G**, and **L** equal 10, 2.5, and 10  $\mu\text{m}$ , respectively.



served in nucleolar islands that represent the dense fibrillar component (Jarrous et al., 1999b) and thus, their passage to nucleoli may be mediated by self-association and/or interaction with another factor present in limiting amounts in the cell. It is noteworthy that both subunits can bind precursor tRNA *in vitro*.

This study reveals that splicing variants of one Rpp subunit may determine the nuclear distribution of another distinct subunit. Thus, expression of exogenous Rpp21i in mouse and human cells causes deformation of nucleoli (Fig. 6A,G) and excludes endogenous Rpp29 from these structures (Fig. 6L–N). Overexpression of Rpp14 and Rpp38 in HeLa cells, for example, does not cause such deformation or exclusion of other subunits from the nucleolus (Jarrous et al., 1999b; data not shown). Physiological roles, for example, control of cell cycle, may be linked to nucleolar distribution of RNase P or its subunits.

### Assembly and function of RNase P in the nucleus

Biochemical studies establish that S100 crude extracts of HeLa cells contain catalytic complexes of human RNase P that are composed of at least nine protein subunits associated with H1 RNA (Eder et al., 1997; Jarrous & Altman, 2001). The findings that H1 RNA (Jacobson et al., 1997) and endogenous Rpp21 are primarily localized in the nucleoplasm, while other subunits, including Rpp14, Rpp29, Rpp38, and hPop1 (Lygerou et al., 1996b), are concentrated in nucleoli may indicate that active RNase P ribonucleoproteins with various subunit stoichiometries may exist in different nuclear compartments of human cells. Alternatively, these individual subunits of RNase P or partial assemblies of the holoenzyme may have functions unrelated to the intact holoenzyme or its activity in the processing of precursor tRNA. For example, Rpp29 and Rpp38 are localized in Cajal bodies, nucleolar-associated structures that are enriched with transcriptosomes and close to transcription sites of U snRNA and histone genes (Frey et al., 1999; Gall et al., 1999).

The localization patterns of the RNA and protein subunits of RNase P indicate that certain subunits are possibly concentrated in nucleoli and Cajal bodies through functional interactions with each other and/or with the transcription apparatus (Lewis & Tollervey, 2000; Pederson, 2000), while some other subunits such as H1 RNA and Rpp21 might be left in the nucleoplasm. Because H1 RNA is dispersed in the nucleus, the assembly of RNase P as a ribonucleoprotein is most likely a dynamic, continuous process in which the subunits are recruited from the nucleoplasm and intranuclear structures to discrete loci of transcription of tRNA genes (Pombo et al., 1999). Some of the subunits, such as Rpp21 and Rpp14, may be recruited by interaction with nascent precursor tRNA. This proposed model for

RNase P formation is compatible with the mechanism ascribed for the passive mobility of proteins and aggregation of RNA processing factors in the nucleus (Lewis & Tollervey, 2000; Pederson, 2000; Phair & Misteli, 2000).

Finally, the distribution of the RNA subunit of nuclear RNase P in human cells is apparently different from that in yeast. In *S. cerevisiae*, the bulk of RNase P RNA is found in the nucleolus and there is evidence that 5' processing of some precursor tRNAs may take place in this structure (Bertrand et al., 1998; Kendall et al., 2000). As in the case with the human holoenzyme, a highly purified RNase P ribonucleoprotein complex with at least nine protein subunits can be obtained from *S. cerevisiae* (Chamberlain et al., 1998). However, a high concentration of a subunit of a ribonucleoprotein complex in a nuclear compartment, such as the nucleolus or Cajal body, does not necessarily reflect the location of the major site of the active holoenzyme (Eils et al., 2000). The lack of typical Cajal bodies in yeast (Gall, 2000) supports this conclusion. The nucleolus and Cajal bodies, and possibly other yet unknown nuclear structures, may primarily serve as assembly, storage, and modification sites for subunits of RNase P in human cells. This concept is strengthened by our finding that inhibition of rDNA gene transcription by low concentration of actinomycin D results in diffusion of Rpp subunits in the nucleoplasm after the collapse of the nucleolar structures and Cajal bodies (N. Jarrous, data not shown). Fully assembled human nuclear RNase P exhibits characteristics of a dynamic ribonucleoprotein that is formed in a transcription-dependent manner.

## MATERIAL AND METHODS

### Molecular cloning of *RPP21* and *RPP21i* cDNAs

The *S. cerevisiae* Rpr2 protein sequence (Chamberlain et al., 1998) was searched in the GenBank database for expressed sequence tag (dbEST) clones using BLAST search programs (Altschul et al., 1997). Several human dbEST clones were found and sequenced. The *RPP21* cDNA used in this study is the I.M.A.G.E. clone #174235 (GenBank accession #H23932) that has an insert of 623 bp with an open reading frame that potentially encodes a polypeptide of 17,570 Da. The GenBank accession number for full-length *RPP21* cDNA is AF212152. *RPP21i* cDNA is an I.M.A.G.E. clone #177912 (GenBank accession #H46800) found to have an insert of 723 bp with an open reading frame encoding a 18,992-Da polypeptide.

### Gene constructs and probes

pHTT7K-Rpp21 was constructed as follows: two primers, one encompassing the ATG translation initiation codon and upstream sequences of *RPP21* cDNA, and the other spanning

the translation stop codon and downstream sequences, were used for PCR with the *RPP21* cDNA as a template. The PCR DNA product was digested with *Bam*H1 (sites are in the designed two primers) and then subcloned downstream from the T7 promoter and in-frame with six histidine residues of pHTT7K that was digested first with *Bam*HI.

The pHTT7K-Rpp21i was constructed as described above for pHTT7K-Rpp21, except that the template for PCR was *RPP21i* cDNA.

pEGFP-Rpp21 was constructed as follows: Rpp21 cDNA (clone #174235) was digested with *Eco*RI and then single-stranded ends were removed by mung bean nuclease. It was then cut with *Not*I and partially filled in by Klenow enzyme using dGTP. The vector pEGFP-C1 was cut with *Eco*RI and then Klenow enzyme was used with dATP to partially fill in the ends, followed by treatment with mung bean nuclease. This was then cut with *Xma*I and Klenow enzyme was used with dCTP to partially fill in the ends. Both pieces were gel purified and ligated. Upon sequencing, we found that the clone was not in-frame, so the plasmid was digested with *Hind*III, filled in, and then self-ligated. This cDNA was confirmed by sequencing to be in-frame with GFP ORF.

pMyc-Rpp21i was constructed by cleaving pMyc-PK with *Eco*RI and *Not*I to first release the chicken pyruvate kinase cDNA. An *RPP21* PCR product, which was generated using two primers encompassing the translation initiation codon and the stop codon of an *RPP21i* cDNA template, was cleaved by *Eco*RI and *Not*I and then subcloned in-frame with the upstream myc-tag sequence.

pEGFP-Rpp21i was constructed by cleaving an *RPP21* PCR product, which was generated using two primers encompassing the translation initiation codon and the stop codon of an *RPP21i* cDNA template, by *Hind*III and *Bam*HI and then subcloned in-frame with GFP in pEGFP-C1 digested first with *Hind*III and *Bam*HI.

An *Eco*RI-*Pst*I cDNA fragment derived from the *RPP21* cDNA was subcloned in pBS (Stratagene) digested with *Eco*RI and *Pst*I and transcribed by T3 RNA polymerase to generate the antisense P3 RNA probe. This 259-bp cDNA fragment covers adjacent exon 1, exon 2, exon 3, and part of exon 4 (Fig. 2C). A 316-bp *Hind*III-*Pst*I cDNA fragment was released from the pEGFP-Rpp21i vector and the isolated insert was subcloned in pBS first digested with *Hind*III and *Pst*I. This cDNA fragment, transcribed by T7 RNA polymerase to synthesize antisense P5 RNA probe, covers adjacent exon 1, intron 1, exon 2, exon 3, and part of exon 4 of the Rpp21i mRNA (Fig. 2C).

The sequence and orientation of all the PCR DNA products and cDNAs used for the construction of the genes and probes described above have been verified by sequencing.

### Cell culture and transfection

Peripheral blood mononuclear cells were separated from buffy coats from healthy donors, washed, and incubated at  $4 \times 10^6$  cells/mL for overnight at 37 °C in RPMI 1640/2% fetal calf serum (Biological Industries, Israel). Human HeLa cells and mouse Swiss 3T3 fibroblasts were grown in high glucose DME (Biological Industries, Israel; Life Technologies, Inc.) and transfected as described (Jarrous et al., 1999b).

### Purification of recombinant Rpp subunits

Overexpression of recombinant Rpp21 and Rpp21i in *E. coli* BL21 (DE3) strain was performed essentially as described (Jarrous et al., 1998). Overexpressed recombinant Rpp21 and Rpp21i proteins were solubilized in 6 M urea. Other recombinant Rpp subunits were overexpressed as previously described (Jarrous et al., 1998, 1999a). After reducing the final concentration of urea to 1 M in binding buffer that contains 5 mM imidazole, all Rpp polypeptides were affinity purified on nickel-charged His-Bind resin chelating columns (Novagen) or a nickel-charged Hi-Trap FPLC column (Amersham-Pharmacia Biotech). Urea was then diluted by extensive dialysis in buffers containing 10 mM Tris-HCl, pH 7.5, 1 mM DTT, 1 mM MgCl<sub>2</sub>, and 5% glycerol. The eluted proteins were separated in PAGE/SDS followed by Coomassie blue or silver staining.

### Gel shift analysis

Five micrograms of highly purified, recombinant Rpp polypeptides were incubated with 5 pmol of internally <sup>32</sup>P-labeled precursor tRNA<sup>Tyr</sup> in binding buffer (150 mM KCl, 2 mM MgCl<sub>2</sub>, 10 mM Tris-HCl, pH 7.5, 1 mM DTT, 5% glycerol). In some experiments, 450 mM of NaCl was included in the binding buffer instead of 150 mM KCl. After 20 min at 25 °C, formation of RNA-protein complexes was tested by retardation in 5% native polyacrylamide gels in TBE×0.5 buffer. Competition was performed in the presence of 100-fold of unlabeled precursor tRNA<sup>Tyr</sup> or poly I:C RNA added to the reaction for 5 min before the addition of the labeled precursor tRNA.

### Antibodies and western blot analysis

Two peptides, NTAHSISDRLPEEKMQTQGSSNQ and VSLRQGFHGDGARRPRVTAPLPQ that correspond to positions 131 to 154 of Rpp21, and to positions 20 to 42 of Rpp21i, respectively, were synthesized and used to raise polyclonal rabbit antibodies. Each peptide was synthesized with a cysteine residue added to its amino terminus to facilitate cross-linking to an activated keyhole limpet hemocyanin (Pierce, Illinois), as an antigen carrier for rabbit immunization. Sera of immunized rabbits were obtained from the Pocono Rabbit Farm and Laboratory (Canadensis, Pennsylvania). The specificity of the antibodies in sera was tested in western blot analysis using crude extracts of HeLa cells. Affinity purified, polyclonal rabbit antibodies against recombinant Rpp29 and Rpp14 have been described (Jarrous et al., 1999a).

Proteins were separated in 12% polyacrylamide/0.1 SDS gels, electrotransferred to a nitrocellulose filter and immunoblotted with a 1:100 dilution of sera (Eder et al., 1997). As a secondary antibody, a 1:5,000 dilution of goat anti-rabbit IgG antibody was used. Blots were washed and antibody-antigen complexes were visualized using the ECL-Plus detection kit (Amersham-Pharmacia Biotech), following the manufacturer's instructions.

### Immunoprecipitation and assay of RNase P

Polyclonal rabbit antibodies (40 μL of sera) were mixed with 5 mg washed protein A Sepharose CL-4B (Amersham Phar-

macia Biotech) in NET-2 buffer (Jarrous et al., 1998). Coupling was made by nutating beads overnight at 4 °C, followed by four washes of beads with NET-2 buffer and two washes with 1×PA buffer that contained 10 U/mL RNasin. Preparations of purified RNase P (10 μL) were added to the beads in a final volume of 150 μL and nutated overnight at 4 °C. Beads were then collected by a short centrifugation and washed several times with 1.5 mL of 1×PA buffer. The immunoprecipitates were then assayed for RNase P activity in processing of the 5' leader of the yeast suppressor precursor tRNA<sup>Ser</sup> (*SupS1*) or *E. coli* precursor tRNA<sup>Tyr</sup> in 1×PA buffer, except that the 1×PA buffer also contained 2 mM Tris-HCl, pH 7.5, 35 mM NaCl, 0.1 mM Na<sub>2</sub>EDTA, 1 mM 2-mercaptoethanol, 0.01% Triton X-100, and 60 U of RNasin.

### Ribonuclease protection analysis

Total RNA was isolated from cells using guanidine thiocyanate/cesium chloride as described (Chirgwin et al., 1979). RNase protection analysis was performed using antisense RNA probes internally labeled with [ $\alpha$ -<sup>32</sup>P]UTP in the presence of cold UTP. RNA (50 μg) was hybridized with 1 × 10<sup>6</sup> cpm of labeled RNA probe in 40 μL buffer A (80% deionized formamide, 40 mM PIPES, pH 6.7, 400 mM NaCl, 1 mM EDTA) for 14 h at 42 °C. RNA was digested for 15 min at 22–25 °C by adding 10 vol of buffer B (10 mM Tris-HCl, pH 7.5, 5 mM EDTA, 300 mM NaCl) that contained 0.8 μg/mL RNase A and 60 U/mL of RNase T1. RNases were then eliminated by Proteinase K/SDS treatment and the protected RNA was extracted with phenol:chloroform and ethanol precipitated in the presence of tRNA. RNA was solubilized in loading buffer (95% formamide, 10 mM Tris-HCl, pH 7.5, 1 mM EDTA), denatured by boiling, and separated in a 4–6% polyacrylamide/urea gel. For single-stranded DNA size marker, pGEM-3 DNA was digested with *MspI* and labeled with [ $\alpha$ -<sup>32</sup>P]dCTP using DNA polymerase I Klenow fragment.

### Immunofluorescence, microscopy, and imaging

Adherent HeLa cells or Swiss 3T3 fibroblasts were grown overnight on coverslips (22 × 22 mm) before fixation for 30 min with 2% formaldehyde (EMS) diluted in 1×PBS. Cells were treated with 0.5% Triton X-100 for 5–30 min, washed twice with 1×PBS (0.5 L each), and blocked with 3% BSA in 1×PBS for 20 min. Rabbit polyclonal antibodies directed against distinct Rpp subunits and p80-coilin (Jarrous et al., 1999b) were diluted 1:50–100 in 3% BSA/PBS, added to the cells for 1 h, and then washed twice with 1×PBS. Alexa<sup>TM</sup> 568 goat anti-rabbit IgG antibody conjugate (Molecular Probes, Inc.) was diluted 1:50 and added to cells for 20 min. When the monoclonal mouse IgG antibodies against anti-fibrillarlin and antimyc (9E10) (Santa Cruz Biotechnology, Inc., California) were included, Alexa<sup>TM</sup> 488 goat anti-mouse IgG antibody conjugate was used as the secondary antibody. Cells were washed twice with 1×PBS and then mounted on glass slides for microscopy.

Confocal fluorescence microscopy of cells was performed as described (Jarrous et al., 1999b). Fluorescent images were acquired by using Texas red and FITC filters, and then processed using LaserSharp software. Bleeding through was

eliminated between fluorophore channels in colocalization studies. Digital processing of images were done using MetaMorph Image acquisition and processing software (Universal Imaging Corp.) and Adobe Photoshop (Adobe Systems, Inc.).

### ACKNOWLEDGMENTS

We thank Joseph Wolenski (Yale University) and Raymond Kaempfer (Hebrew University) for assistance and discussions. This work is supported by U.S. Public Health Service Grant GM 19422 and Human Frontier of Science Program Grant RG-02N1 1997M to S. Altman, and by the Leszynski Fund for Advanced Research to N. Jarrous. N. Jarrous is the recipient of a Kahanoff Foundation fellowship.

Received April 2, 2001; returned for revision April 27, 2001; revised manuscript received May 8, 2001

### REFERENCES

- Altman S, Kirsebom L. 1999. Ribonuclease P. In: Gesteland RF, Cech T, Atkins JF, eds. *The RNA world*. Cold Spring Harbor, New York: Cold Spring Harbor Laboratory Press. pp 351–380.
- Altschul SF, Madden TL, Schaffer AA, Zhang J, Zhang Z, Miller W, Lipman DJ. 1997. Gapped BLAST and PSI-BLAST: A new generation of protein database search programs. *Nucleic Acids Res* 25:3389–3402.
- Beinert H, Kiley PJ. 1999. Fe-S proteins in sensing and regulatory functions. *Curr Opin Chem Biol* 3:152–157.
- Bertrand E, Houser-Scott F, Kendall A, Singer RH, Engelke DR. 1998. Nucleolar localization of early tRNA processing. *Genes & Dev* 12:2463–2468.
- Braud VM, Allan DS, O'Callaghan CA, Soderstrom K, D'Andrea A, Ogg GS, Lazetic S, Young NT, Bell JI, Phillips JH, Lanier LL, McMichael AJ. 1998. HLA-E binds to natural killer cell receptors CD94/NKG2A, B and C. *Nature* 391:795–799.
- Chamberlain JR, Lee Y, Lane WS, Engelke DR. 1998. Purification and characterization of the nuclear RNase P holoenzyme complex reveals extensive subunit overlap with RNase MRP. *Genes & Dev* 12:1678–1690.
- Chirgwin JM, Przybyla AE, MacDonald RJ, Rutter WJ. 1979. Isolation of biologically active ribonucleic acid from sources enriched in ribonuclease. *Biochemistry* 18:5294–5299.
- Chu S, Zengel JM, Lindahl L. 1997. A novel protein shared by RNase MRP and RNase P. *RNA* 3:382–391.
- Coldren CD, Hellinga HW, Caradonna JP. 1997. The rational design and construction of a cuboidal iron-sulfur protein. *Proc Natl Acad Sci USA* 94:6635–6640.
- Dichtl B, Tollervey D. 1997. Pop3p is essential for the activity of the RNase MRP and RNase P ribonucleoproteins in vivo. *EMBO J* 16:417–429.
- Eder PS, Kekuda R, Stolc V, Altman S. 1997. Characterization of two scleroderma autoimmune antigens that copurify with the ribonucleoprotein ribonuclease P. *Proc Natl Acad Sci USA* 94:1101–1106.
- Eils R, Gerlich D, Tvarusko W, Spector DL, Misteli T. 2000. Quantitative imaging of pre-mRNA splicing factors in living cells. *Mol Biol Cell* 11:413–418.
- Frank DN, Pace NR. 1998. Ribonuclease P: Unity and diversity in a tRNA processing ribozyme. *Annu Rev Biochem* 67:153–180.
- Frey MR, Bailey AD, Weiner AM, Matera AG. 1999. Association of snRNA genes with coiled bodies is mediated by nascent snRNA transcripts. *Curr Biol* 9:126–135.
- Gall JG. 2000. Cajal bodies: The first 100 years. *Annu Rev Cell Dev Biol* 16:273–300.
- Gall JG, Bellini M, Wu Z, Murphy C. 1999. Assembly of the nuclear transcription and processing machinery: Cajal bodies (coiled bodies) and transcriptosomes. *Mol Biol Cell* 10:4385–4402.

- Gold HA, Topper JN, Clayton DA, Craft J. 1989. The RNA processing enzyme RNase MRP is identical to the Th RNP and related to RNase P. *Science* 245:1377–1380.
- Gruen JR, Nalabolu SR, Chu TW, Bowlus C, Fan WF, Goei VL, Wei H, Sivakamasundari R, Liu Y, Xu HX, Parimoo S, Nallur G, Ajioka R, Shukla H, Bray-Ward P, Pan J, Weissman SM. 1996. A transcription map of the major histocompatibility complex (MHC) class I region. *Genomics* 36:70–85.
- Hodgkinson AD, Millward BA, Demaine AG. 2000. The HLA-E locus is associated with age at onset and susceptibility to type 1 diabetes mellitus. *Hum Immunol* 61:290–295.
- Jacobson MR, Cao LG, Taneja K, Singer RH, Wang YL, Pederson T. 1997. Nuclear domains of the RNA subunit of RNase P. *J Cell Sci* 110:829–837.
- Jarrous N, Altman S. 2001. Human ribonuclease P. *Methods Enzymol* 342:93–100.
- Jarrous N, Eder PS, Guerrier-Takada C, Hoog C, Altman S. 1998. Autoantigenic properties of some protein subunits of catalytically active complexes of human ribonuclease P. *RNA* 4:407–417.
- Jarrous N, Eder PS, Wesolowski D, Altman S. 1999a. Rpp14 and Rpp29, two protein subunits of human ribonuclease P. *RNA* 5:153–157.
- Jarrous N, Wolenski JS, Wesolowski D, Lee C, Altman S. 1999b. Localization in the nucleolus and coiled bodies of protein subunits of the ribonucleoprotein ribonuclease P. *J Cell Biol* 146:559–572.
- Kendall A, Hull MW, Bertrand E, Good PD, Singer RH, Engelke DR. 2000. A CBF5 mutation that disrupts nucleolar localization of early tRNA biosynthesis in yeast also suppresses tRNA gene-mediated transcriptional silencing. *Proc Natl Acad Sci USA* 97:13108–13113.
- Lamond AI, Earnshaw WC. 1998. Structure and function in the nucleus. *Science* 280:547–553.
- Lee B, Matera AG, Ward DC, Craft J. 1996. Association of RNase mitochondrial RNA processing enzyme with ribonuclease P in higher ordered structures in the nucleolus: A possible coordinate role in ribosome biogenesis. *Proc Natl Acad Sci USA* 93:11471–11476.
- Lee DY, Clayton DA. 1997. RNase mitochondrial RNA processing correctly cleaves a novel R loop at the mitochondrial DNA leading-strand origin of replication. *Genes & Dev* 11:582–592.
- Lewis JD, Tollervey D. 2000. Like attracts like: Getting RNA processing together in the nucleus. *Science* 288:1385–1389.
- Lygerou Z, Allmang C, Tollervey D, Séraphin B. 1996a. Accurate processing of a eukaryotic precursor ribosomal RNA by ribonuclease MRP in vitro. *Science* 272:268–270.
- Lygerou Z, Mitchell P, Petfalski E, Séraphin B, Tollervey D. 1994. The POP1 gene encodes a protein component common to the RNase MRP and RNase P ribonucleoproteins. *Genes & Dev* 8:1423–1433.
- Lygerou Z, Pluk H, van Venrooij WJ, Séraphin B. 1996b. hPop1: An autoantigenic protein subunit shared by the human RNase P and RNase MRP ribonucleoproteins. *EMBO J* 15:5936–5948.
- Matera AG, Frey MR, Margelot K, Wolin SL. 1995. A perinucleolar compartment contains several RNA polymerase III transcripts as well as the polypyrimidine tract-binding protein, hnRNP I. *J Cell Biol* 129:1181–1193.
- Pederson T. 2000. Diffusional protein transport within the nucleus: A message in the medium. *Nature Cell Biol* 2:E73–E74.
- Pederson T, Politz JC. 2000. The nucleolus and the four ribonucleoproteins of translation. *J Cell Biol* 148:1091–1095.
- Pfeiffer T, Tekos A, Warnecke JM, Drinas D, Engelke DR, Séraphin B, Hartmann RK. 2000. Effects of phosphorothioate modifications on precursor tRNA processing by eukaryotic RNase P enzymes. *J Mol Biol* 298:559–565.
- Phair RD, Misteli T. 2000. High mobility of proteins in the mammalian cell nucleus. *Nature* 404:604–609.
- Pluk H, van Eenennaam H, Rutjes SA, Pruijn GJ, van Venrooij WJ. 1999. RNA–protein interactions in the human RNase MRP ribonucleoprotein complex. *RNA* 5:512–524.
- Pombo A, Jackson DA, Hollinshead M, Wang Z, Roeder RG, Cook PR. 1999. Regional specialization in human nuclei: Visualization of discrete sites of transcription by RNA polymerase III. *EMBO J* 18:2241–2253.
- Shaw PJ, Highett MI, Beven AF, Jordan EG. 1995. The nucleolar architecture of polymerase I transcription and processing. *EMBO J* 14:2896–2906.
- Shiina T, Tamiya G, Oka A, Takishima N, Yamagata T, Kikkawa E, Iwata K, Tomizawa M, Okuaki N, Kuwano Y, Watanabe K, Fukuzumi Y, Itakura S, Sugawara C, Ono A, Yamazaki M, Tashiro H, Ando A, Ikemura T, Soeda E, Kimura M, Bahram S, Inoko H. 1999. Molecular dynamics of MHC genesis unraveled by sequence analysis of the 1,796,938-bp HLA class I region. *Proc Natl Acad Sci USA* 96:13282–13287.
- Stolc V, Altman S. 1997. Rpp1, an essential protein subunit of nuclear RNase P required for processing of precursor tRNA and 35S precursor rRNA in *Saccharomyces cerevisiae*. *Genes & Dev* 11:2926–2937.
- Stolc V, Katz A, Altman S. 1998. Rpp2, an essential protein subunit of nuclear RNase P, is required for processing of precursor tRNAs and 35S precursor rRNA in *Saccharomyces cerevisiae*. *Proc Natl Acad Sci USA* 95:6716–6721.
- Thomas BC, Chamberlain J, Engelke DR, Gegenheimer P. 2000. Evidence for an RNA-based catalytic mechanism in eukaryotic nuclear ribonuclease P. *RNA* 6:554–562.
- van Eenennaam H, Pruijn GJ, van Venrooij WJ. 1999. hPop4: A new protein subunit of the human RNase MRP and RNase P ribonucleoprotein complexes. *Nucleic Acids Res* 27:2465–2472.
- Wolin SL, Matera AG. 1999. The trials and travels of tRNA. *Genes & Dev* 13:1–10.